⌘ *Author's Choice*

THE JOURNAL OF BIOLOGICAL CHEMISTRY VOL. 286, NO. 10, pp. 8577–8584, March 11, 2011

Cooperativeness of Orai Cytosolic Domains Tunes Subtype-specific Gating*[S]

Received for publication, September 21, 2010, and in revised form, December 23, 2010 Published, JBC Papers in Press, January 10, 2011, DOI 10.1074/jbc.M110.187179

Irene Frischauf[‡1,2], Rainer Schindl[‡1,3], Judith Bergsmann[‡1,4], Isabella Derler[‡5], Marc Fahrner[‡], Martin Muik[‡], Reinhard Fritsch[‡], Barbara Lackner[‡], Klaus Groschner[§], and Christoph Romanin[‡6]

From the [‡]Institute of Biophysics, University of Linz, Altenbergerstrasse 69, 4040 Linz, Austria and the [§]Department of Pharmaceutical Sciences-Pharmacology and Toxicology, University of Graz, Universitätsplatz 2, 8010 Graz, Austria

Activation of immune cells is triggered by the Ca^{2+} release-activated Ca^{2+} current, which is mediated via channels of the Orai protein family. A key gating process of the three Orai channel isoforms to prevent Ca^{2+} overload is fast inactivation, most pronounced in Orai3. A subsequent reactivation is a unique gating characteristic of Orai1 channels, whereas Orai2 and Orai3 currents display a second, slow inactivation phase. Employing a chimeric approach by sequential swapping of respective intra- and extracellular regions between Orai1 and Orai3, we show here that Orai1 specific proline/arginine-rich domains in the N terminus mediate reactivation, whereas the second, intracellular loop modulates fast and slow gating processes. Swapping C-terminal strands lacks a significant impact. However, simultaneous transfer of Orai3 N terminus and its second loop or C terminus in an Orai1 chimera substantially increases fast inactivation centered between wild-type channels. Concomitant swap of all three cytosolic strands from Orai3 onto Orai1 fully conveys Orai3-like gating characteristics, in a strongly cooperative manner. In conclusion, Orai subtype-specific gating requires a cooperative interplay of all three cytosolic domains.

Ca^{2+} entry through store-operated channels is, among other mechanisms, an ubiquitous and fundamental way of cell signaling (1). Initialized by a signaling cascade generating inositol 1,4,5-trisphosphate, the ensuing Ca^{2+} depletion from the endoplasmic reticulum is sensed by the stromal interaction molecule STIM1 (2, 3). Subsequently, STIM1 assembles into higher order aggregates and migrates into defined regions close to the plasma membrane (4). At these oligomerized STIM1 hotspots, interaction with the membrane protein Orai1 occurs thereby activating the Ca^{2+}-selective Ca^{2+} release-activated Ca^{2+} current, which belongs to the best characterized store-operated channels (5–8).

Accurate control of activation and inactivation of Ca^{2+} channels is a prerequisite for correct cell function, as Ca^{2+} overload might lead to apoptosis. Such a control is accomplished by a negative feedback mechanism termed Ca^{2+}-dependent inactivation, which limits Ca^{2+} inward currents. This process is triggered by cytoplasmic Ca^{2+} close (3–4 nm) to the pore mouth of the channels (9, 10).

Ca^{2+}-dependent inactivation is most pronounced in Orai3 currents compared with Orai1 or Orai2. A unique characteristic of Orai1 channels is a subsequent slow reactivation, whereas Orai2 and Orai3 currents continue with a slow inactivation phase (11, 12).

Independent studies have identified several regions within STIM1 and Orai that contribute to the fast inactivation phase. In particular, Ca^{2+}-dependent inactivation is controlled by negatively charged residues within the outer pore vestibule of Orai1 channels (13). Furthermore, a membrane proximal N-terminal domain in Orai1 has been reported to interact with the Ca^{2+} binding protein calmodulin (14). Mutations that abrogate calmodulin binding have substantially reduced Ca^{2+}-dependent inactivation (14). Additionally, a central region within the second loop of Orai1 is essential for the fast inactivation process of Ca^{2+} release-activated Ca^{2+} channels. Expression of a peptide comprising the second loop inhibits Orai1 channel activity, suggesting this domain as inactivation particle (15). Fast inactivation of Orai2 and Orai3 channels has been attributed to three conserved glutamates in their C termini (16). Within STIM1, an acidic cluster (amino acids 475–483) has been shown to modulate fast inactivation (14, 16, 17).

Although these reports uncovered several Orai regions involved in inactivation, subtype-specific Orai domains leading to their distinct gating profiles have not yet been identified. By using domain swapping between Orai1 and Orai3, this study enabled the identification of unique structures for both inactivation and reactivation. Moreover, we uncovered cooperativeness among cytosolic domains that accomplish the Orai subtype-specific gating.

EXPERIMENTAL PROCEDURES

Molecular Cloning and Mutagenesis—Human pECFP-C1 and pEYFP-C1 Orai1, Orai3, and STIM1 were described previously (5, 18). Human Orai2 (accession no. NM_032831) kindly provided by L. Birnbaumer (NIEHS, National Institutes of Health) was subcloned into pECFP-C1 and pEYFP-C1 using KpnI and XbaI. All point mutations and deletions in Orai constructs were generated using the site-directed mutagenesis kit from Stratagene. Orai1 and Orai3 chimera were amplified via splicing by overlap extensions and subcloned via internal

* This work was supported in part by Austrian Science Foundation (FWF) Projects P22747 (to R. S.), P211925 (to K. G.), and P21118 (to C. R.).

⌘ *Author's Choice*—Final version full access.

[S] The on-line version of this article (available at http://www.jbc.org) contains supplemental Figs. S1–S5.

[1] These authors contributed equally to this work.

[2] Recipient of Hertha-Firnberg Scholarship T442.

[3] To whom correspondence may be addressed. E-mail: rainer.schindl@jku.at.

[4] Recipient of a scholarship from the Austrian Academy of Sciences.

[5] Recipient of Hertha-Firnberg Scholarship T466.

[6] To whom correspondence may be addressed. E-mail: christoph.romanin@jku.at.

restriction sites BamHI and XbaI into pECFP-C1 and pEYFP-C1. The integrity of all clones was confirmed by sequence analysis (VBC, Vienna).

Whole Cell Recordings—Cells transfected (Transfectin, Bio-Rad) with 1 μg DNA of Orai and STIM1 constructs were identified by CFP[7]/YFP/Cherry fluorescence. All Orai constructs were tested for a correct plasma membrane expression. Where indicated, 2 μg DNA of STIM1 and 0.5 μg DNA of Orai1 chimeras were used. Electrophysiological experiments were performed at 21–25 °C, using the patch clamp technique in whole cell recording configurations. An Ag/AgCl electrode was used as reference electrode. For STIM1- and Orai1/Orai3-mediated currents, voltage ramps were applied every 5 s from a holding potential of 0 mV, covering a range of −90 to 90 mV for 1 s. Upon maximum activation, voltage steps from −90, −70, −50 to −30 mV for 2 s were applied every 5 s from a holding potential of 0 mV. The internal pipette solution designed for passive store depletion of Orai-derived currents contained the following: 145 mM cesium methane sulfonate, 8 mM NaCl, 3.5 mM $MgCl_2$, 10 mM HEPES, 10 mM EGTA, pH 7.2. The standard extracellular solution consisted of 145 mM NaCl, 5 mM CsCl, 1 mM $MgCl_2$, 10 mM HEPES, 10 mM glucose, 10 mM $CaCl_2$, pH 7.4. Applied potentials were corrected for a liquid junction of +12 mV resulting from a Cl^--based bath solution and a sulfonate-based pipette solution. All currents are leak subtracted either by subtracting the initial voltage ramps obtained shortly following break-in with no visible current activation or the remaining currents after 10 μM La^{3+} application at the end of the experiment, with both yielding identical results.

Fluorescence Microscopy—Confocal FRET microscopy was performed similarly as described in Ref. 19. In brief, a QLC100 real-time confocal system (VisiTech Int.) was used for recording fluorescence images connected to two Photometrics CoolSNAPHQ monochrome cameras (Roper Scientific) and a dual port adapter (dichroic, 505 lp; cyan emission filter, 485/30; yellow emission filter, 535/50; Chroma Technology Corp.). This system was attached to an Axiovert 200 M microscope (Zeiss, Germany) in conjunction with an argon ion multi-wavelength (457, 488, and 514 nm) laser (Spectra Physics). The wavelengths were selected by an Acousto Optical Tuneable Filter (VisiTech Int.). MetaMorph software (version 5.0, Universal Imaging Corp.) was used to acquire images and to control the confocal system. Illumination times of ~900–1500 ms were typically used for CFP, FRET, and YFP images that were consecutively recorded with a minimum delay. Prior to calculation, the images had to be corrected due to cross-talk as well as cross-excitation. For this, the appropriate cross-talk calibration factors were determined for each of the constructs on the day the FRET experiments were performed. The corrected FRET image (N_{FRET}) was calculated on a pixel-to-pixel basis after background subtraction and threshold determination using a custom-made software (20) integrated in MatLab (version 7.0.4) according to the method published by (21). The local ratio between CFP and YFP might vary due to different localizations of diverse protein constructs, which could lead to the calculation of false FRET values (22). Accordingly, the analysis was limited to pixels with a CFP:YFP molar ratio between 1:10 and 10:1 to yield reliable results (22).

[7] The abbreviations used are: CFP, cyan fluorescent protein; YFP, yellow fluorescent protein; Nt, N terminus; Ct, C terminus; CaM, calmodulin.

RESULTS

Inactivation and Reactivation Profiles of Three Orai Channel Isoforms—We examined whether the divergent gating properties of the three Orai1/2/3 channels can be pinpointed to unique structural features within these proteins. Co-expression of STIM1 with each of the Orai proteins in HEK cells resulted in inwardly rectifying Ca^{2+} currents following passive store depletion by 20 mM EGTA in the pipette solution (12). Upon maximum activation of Orai currents, voltage steps from a holding potential of 0 mV to −82 mV over 1800 ms enabled to monitor gating characteristics represented by both inactivation and reactivation phases (Fig. 1*D*). In a simplified, quantitative evaluation, we separated fast inactivation (both Orai1 and Orai3) from slow reactivation (Orai1) or inactivation (Orai3) in the following manner. Normalized, residual currents were calculated for a time point at 100 ms representing fast inactivation (Fig. 1*E*), and slow inactivation/reactivation was estimated by subtracting normalized currents at 1500 ms from those at 100 ms (Fig. 1*F*) as graphically presented in Fig. 1*D*.

Within a time frame of 100 ms, normalized, residual Ca^{2+} currents of Orai1 (Fig. 1*B* and supplemental Fig. S1*A*) and of Orai2 (supplemental Fig S1*A*) yielded a similar moderate, fast inactivation to ~ 0.8 of initial peak values. In contrast, fast inactivation of Orai3 currents was more pronounced and reached ~0.45 of initial values at the first 100 ms (Fig. 1*B* and supplemental Fig. S1*A*). Following the fast inactivation, Orai1 (Fig. 1*C*) exhibited a subsequent phase of reactivation, whereas Orai2 (supplemental Fig. S1*B*) and Orai3 (Fig. 1*C*) currents progressed with a slower inactivation. The separation in fast and slow gating processes was further supported by their distinct Ca^{2+} dependence (supplemental Fig. S1, *C–F*). Fast inactivation was clearly a Ca^{2+}-mediated process in both Orai1/3 isoforms, whereas slow reactivation/inactivation appeared Ca^{2+}-independent (supplemental Fig. S1, *C–F*), evaluated by a Ba^{2+}- instead of Ca^{2+}-containing extracellular solution.

In this study, we focused on distinct intracellular as well as extracellular domains within Orai1 and Orai3 channels as their inactivation/reactivation profiles are most divergent. For identification of domains mediating specific Orai-gating characteristics, chimeras were generated initially by single domain swaps and later on extended to double or triple domain exchanges between Orai1 and Orai3.

Proline/Arginine-rich Regions in Orai1 N Terminus Contribute to Orai Reactivation Phase—The whole Orai1 N-terminal domain was substituted by that of Orai3 (termed O1-[Nt-O3]). The inactivation profile of O1-[Nt-O3] exhibited a similar modest fast inactivation as wild-type Orai1 (Fig. 1*B*), followed by a decreased reactivation (Fig. 1*C*). Reciprocally, an Orai3 chimera with the N terminus of Orai1 (O3-[Nt-O1]) led to reduction of fast inactivation (Fig. 1*B*) and the appearance of a reactivation phase typical of wild-type Orai1 (Fig. 1*C*). These findings suggest that the N terminus of Orai1 plays a substantial role in the reactivation process. To address the essential domains within the N terminus involved in reactivation of

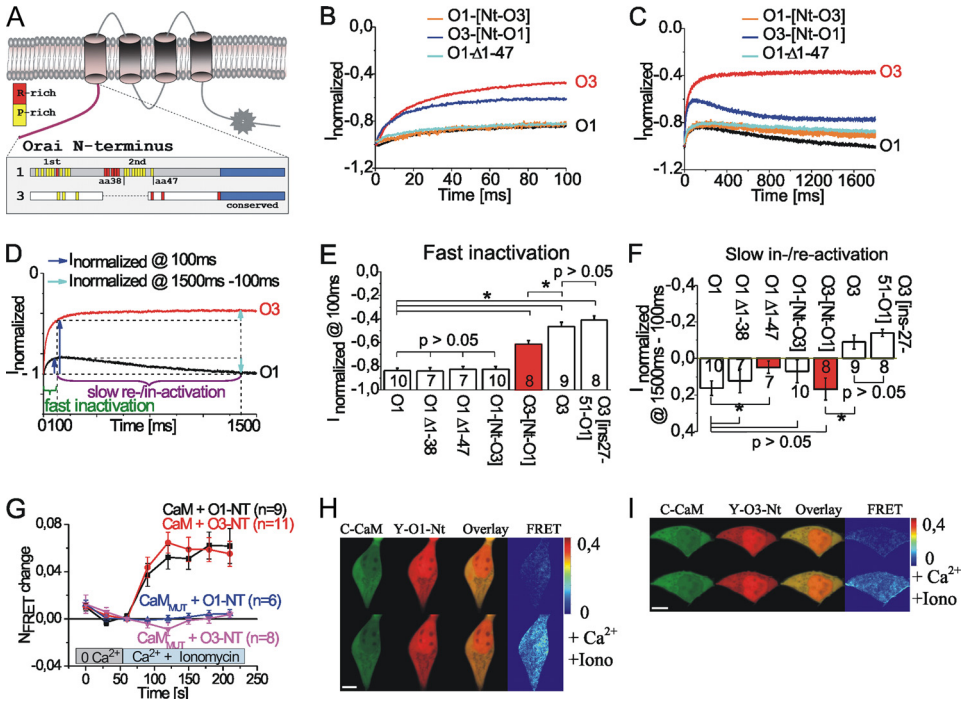

FIGURE 1. **The proline/arginine-rich regions of the Orai1 N terminus mediate reactivation.** *A*, a scheme depicts an Orai protein with its four transmembrane segments and highlights the unique arginine/proline/arginine-rich region within Orai1. *R*, Arg; *P*, Pro. *B* and *C*, normalized average currents from a voltage step to −82 mV are shown for a coexpression of STIM1 with Orai1 (*O1*, *black*), Orai3 (*O3*, *red*), as well as O1-[Nt-O3], O3-[Nt-O1], or O1-Δ1–47 for 100 (*B*) or 1800 (*C*) ms. *D*, normalized average currents were calculated for a time point at 100 ms representing fast inactivation (*blue arrows*) and slow inactivation/reactivation (*cyan arrows*) was estimated by subtracting normalized currents at 1500 ms from those at 100 ms. *E* and *F*, statistics on normalized average currents ± S.E. compare O1, O1-Δ1–38, O1-Δ1–47, O1-[NT-O3], O3-[NT-O1], O3, and O3-[ins27–51-O1] at 100 (*E*) and 1500–100 ms (*F*). *G*, time course of average FRET change ± S.E. between CFP-CaM or CFP-CaM$_{MUT}$ and YFP-O1-Nt or YFP-O3-Nt in response to addition of 10 μM ionomycin (*Iono*) and 2 mM Ca^{2+} in a bath solution administered at 1 min. At 3 min, the relative FRET values of YFP-O1-Nt or YFP-O3-Nt coexpressed with CFP-CAM is significantly different ($p < 0.01$) to a coexpression of either Orai-Nt with the CaM$_{MUT}$. *H* and *I*, localization, overlay, and calculated FRET life cell image series of CFP-CaM and YFP-Orai1-Nt (*H*) or YFP-Orai3-Nt (*I*) in a nominally Ca^{2+} extracellular solution (*upper images*) or with 2 mM Ca^{2+} and 10 μM ionomycin added (*lower images*).

Orai1, we focused on the initial stretch less conserved between Orai isoforms. This Orai1 region includes two proline-rich domains with five arginines in between (Fig. 1*A*). Deletion of the whole N-terminal proline/arginine-rich portion in Orai1 (O1-Δ1–47) almost abolished reactivation (Fig. 1*C*), resulting in a similar inactivation/reactivation profile as that of O1-[Nt-O3]. This deletion mutant also lacked the Orai1-type reactivation phase in a Ba^{2+} solution and yielded constant inward-currents >1500 ms (supplemental Fig. S1*H*).

A shorter truncation of the first proline, together with the arginine-rich domain in Orai1 (O1-Δ1–38), retained inactivation/reactivation similar to wild-type Orai1 (Fig. 1*F*). In addition, introduction of the arginine-rich and the second proline-rich segment of O1 (amino acids 27–51) into a corresponding site (between amino acids 26 and 27) of Orai3 N terminus (O3-[ins27–51-O1]) did not markedly alter Orai3 slow inactivation profile (Fig. 1*F*). Therefore, these experiments suggest that the whole proline/arginine-rich region of Orai1 is required to confer the reactivation phase in an Orai3 chimera, whereas the second proline-rich segment is sufficient for Orai1.

Conserved Coupling of Calmodulin to Orai1 and Orai3 N Termini—A membrane-adjacent N-terminal stretch of ~40 residues is well conserved in Orai proteins and coimmunoprecipitates with calmodulin (CaM) in the presence of Ca^{2+} (14). Orai1 mutants with eliminated CaM binding exhibited abrogated fast inactivation (14). We investigated interaction of CFP-labeled calmodulin or a Ca^{2+}-insensitive mutant (CaM$_{MUT}$) with the YFP N termini of Orai1 and Orai3 by FRET microscopy. At resting cytosolic Ca^{2+} levels, no FRET was detected for the N termini of Orai1 (Orai1-NT, Fig. 1, *G* and *H*) or Orai3 (Fig. 1, *G* and *I*) with CaM. Addition of 2 mM extracellular Ca^{2+} solution and 10 μM ionomycin increased cytosolic Ca^{2+} levels and resulted in a similar interaction of both Orai N-terminal fragments with CaM (Fig. 1, *G--I*). CaM$_{MUT}$ lacked coupling to both Orai N termini independent of Ca^{2+} levels (Fig. 1*G*). Hence, the interaction of CaM with Orai1 and Orai3 is similar and therefore not expected to cause Orai sub-type specific gating.

Second Loop Modulates Fast and Slow Inactivation—Orai1 gating is also determined by the second intracellular loop. It has been shown that alanine substitutions at a central region within this loop abolish fast inactivation (15). An Orai3 chimera with the second loop substituted by that of Orai1 (O3-[L2-O1]) showed a substantial reduction of fast inactivation in comparison to wild-type Orai3 (Fig. 2*B*). Fast inactivation was modest similar to that of Orai1 (Fig. 2, *B* and *D*), with a subsequent unique slow inactivation phase (Fig. 2, *C* and *E*). Orai3-[L2-O1]-mediated Ba^{2+} currents lack both fast (supplemental Fig. S2*A*) and slow inactivation phase (supplemental Fig. S2*B*), suggesting that this novel slow inactivation is also Ca^{2+}-dependent.

In contrast, substitution of the second loop of Orai1 by that of Orai3 (O1-[L2-O3]) failed to significantly affect fast inactivation (Fig. 2, *B* and *D*) and reactivation (Fig. 2, *C* and *E*) in

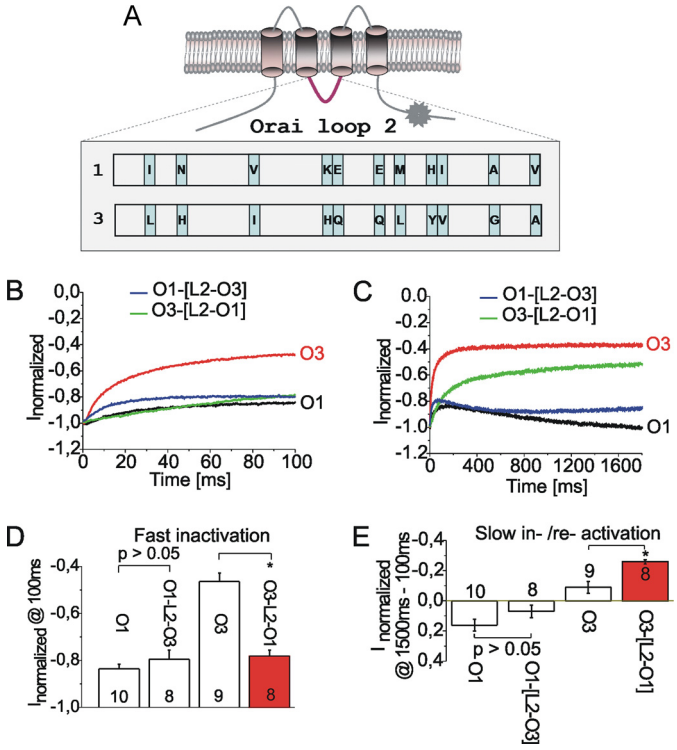

FIGURE 2. **The second loop of Orai1 transferred into Orai3 reduces fast inactivation.** *A*, the scheme depicts an Orai protein and highlights nonconserved residues within the second loop of Orai1 or Orai3. *B* and *C*, normalized average currents from a voltage step to −82 mV are shown for a coexpression of STIM1 with O1 (*black*), O3 (*red*), as well as O1-[L2-O3] and O3-[L2-O1] for 100 (*B*) or 1800 (*C*) ms. *D* and *E*, statistics on normalized average currents ± S.E. compare O1, O1-[L2-O3], O3, and O3-[L2-O1] at 100 (*D*) and 1500–100 (*E*) ms.

comparison with wild-type Orai1. As the reciprocal domain swap from Orai3 into Orai1 did not confer Orai3-like strong inactivation, these experiments suggest that corresponding domains within Orai proteins have either distinct roles or more likely do not act independent but function within the context of the whole Orai1/3 channel complex.

In a further effort to pinpoint those nonconserved amino acids (Fig. 2*A*) within the second loop of Orai1 that conferred the reduction of fast inactivation into Orai3, we generated various Orai3 constructs with single or double point mutations in the second loop (Fig. 2*A* and supplemental Fig. S2, *C* and *D*). However, none of those significantly reduced fast inactivation as observed with the O3-[L2-O1] chimera (supplemental Fig. S2*C*), and contribution to the slower gating process appeared more complex, as mutants exhibited either increased slow inactivation or even a reactivation phase (supplemental Fig. S2*D*).

Orai3-specific Extensions in Third Loop Modulate Inactivation Profile—The third extracellular loop has not yet been investigated, considering its impact on gating characteristics. Besides extensions in Orai1 N and C termini, this loop comprises Orai3-specific large insertions. Adjacent to transmembrane segment III, Orai3 consists of a 25-residue-long stretch, followed by a unique short (amino acids 199–206 in Orai3) and a longer (amino acids 217–239) insertion, as well as 12 highly conserved amino acids (amino acids 240–251) (Fig. 3*A*). For the preparation of deletion mutants, we separated this unique region into two stretches (amino acids 199–217 and amino acids 218–239). Deletion of the first stretch (Orai3-Δ199–217) did neither significantly alter fast (Fig. 3, *B* and *D*) and slow inactivation (Fig. 3, *C* and *E*) in comparison with wild-type Orai3. An Orai3 mutant lacking the second stretch (Orai3-Δ218–239) showed a clear reduction in fast inactivation (Fig. 3, *B* and *D*), whereas slow inactivation was more pronounced (Fig. 3, *C* and *E*). A shorter Orai3 deletion within this latter stretch (Orai3-Δ218–234) also enhanced slow inactivation (Fig. 3, *B* and *D*), whereas fast inactivation remained almost unchanged compared with wild-type Orai3 (Fig. 3, *C* and *E*). Hence, the second stretch within the insert of the third extracellular loop of Orai3 is able to modulate gating characteristics with residues 235–239 contributing to Orai3-specific fast inactivation.

C Termini Swaps Do Not Affect Gating Characteristics—Fast inactivation of Orai2 and Orai3 channels has been attributed to three conserved glutamates in their C termini, whereas one glutamate out of these three is an aspartate in Orai1 (16). Glutamate-to-alanine substitutions within Orai3 dramatically reduce fast inactivation (16). The C terminus of Orai1 includes a putative coiled-coil domain required for STIM1 coupling (23) as well as a unique 12-residue-long extension at its end (Fig. 3*A*). To examine a subtype-specific gating effect, we generated an Orai1 chimera with the C terminus of Orai3 (O1-[Ct-O3]). Although fast inactivation was unaffected (Fig. 3, *F* and *H*), reactivation appeared reduced but not to a significant extent (Fig. 3, *G* and *I*). Vice versa, Orai3 with a substituted C terminus of Orai1 (O3-[Ct-O1]) did not show altered gating characteristics compared with wild-type Orai3 (Fig. 3, *F–I*).

The coiled-coil domains in Orai1 and Orai3 are only partially conserved (23). Although the coupling of the Stim1 C terminus to Orai1 is abolished by a single coiled-coil mutation in the C terminus of the channel (5), a similar Orai3 mutation (Orai3-L285S) only reduces this coupling (23). We determined whether a reduced Stim1 coupling to Orai3 coiled-coil mutants affects their inactivation profiles. Upon store depletion by 60 μM 2,5-di-(tert-butyl)-1,4-benzohydro-quinone, the coiled-coil mutants YFP-Orai3-L285S and CFP-Orai3-L292S co-expressed with CFP-/YFP-Stim1 yielded an ~35 and 20% FRET reduction in comparison with the respective WT-Orai3 and Stim1 (supplemental Fig. S3*A*). Inactivation steps of Orai3-L292S remained unaffected compared with WT-Orai3 (supplemental Fig. S3, *B–E*). Orai3-L285S also yielded a similar fast inactivation phase (supplemental Fig. S3, *B* and *D*), whereas the slow inactivation phase was further increased (supplemental Fig. S3, *C* and *E*). Hence, these experiments clearly show that a reduced Stim1 coupling to Orai3 mutants does not reduce inactivation indicating the prevalence of cytosolic domains over STIM1 in the control of inactivation.

Besides a general role of the conserved glutamates in inactivation of Orai channels (16), swaps of C termini and coiled-coil mutations did not substantially affect Orai1 and Orai3 inactivation/reactivation profiles suggesting the requirement of additional domains to confer subtype-specific gating characteristics.

Cooperativeness of Orai Cytosolic Gating Domains—The results obtained so far indicate that Orai1 chimeras with a single N and C terminus or second loop substitution from Orai3 exhibited only slight and no substantial increases in fast inactivation as present in Orai3 (Fig. 4, *A* and *B*). These experiments

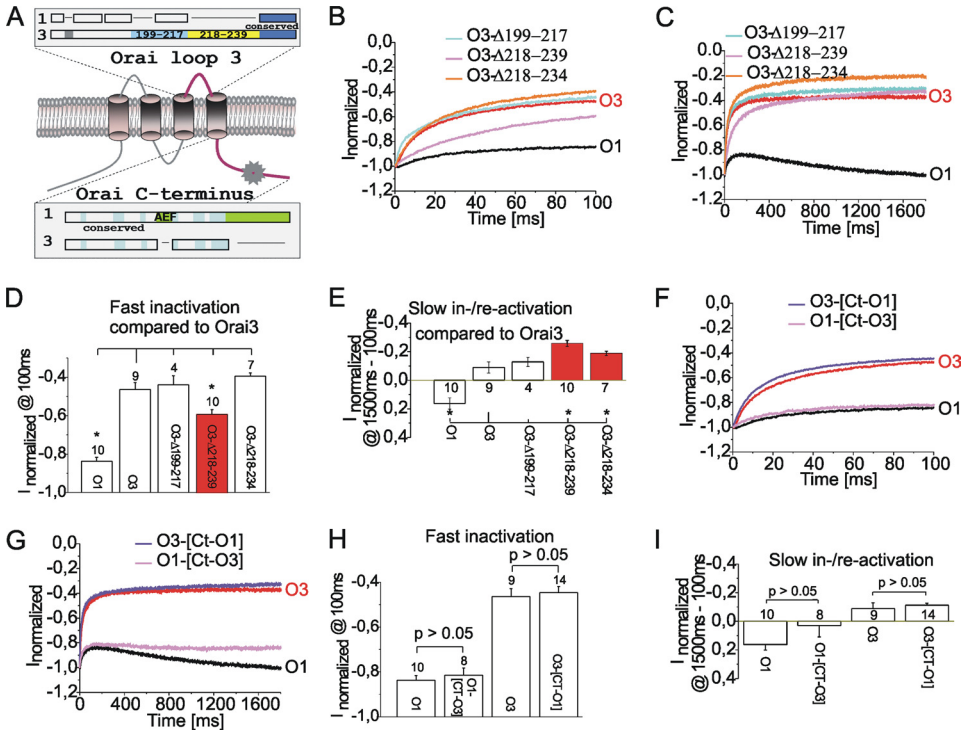

FIGURE 3. **Effect of the third loop and the C terminus on Orai gating.** *A*, the scheme depicts an Orai protein and highlights unique insertions within the third loop of Orai3 as well as C terminus of Orai1. *B* and *C*, normalized average currents from a voltage step to −82 mV are shown for a coexpression of STIM1 with O1 (*black*), O3 (*red*), as well as O3-Δ199–217, O3-Δ218–239, and O3-Δ218–234 for 100 (*B*) or 1800 (*C*) ms. Statistics on normalized average currents ± S.E. compare O1, O3, O3-Δ199–217, O3-Δ218–239, and O3-Δ218–234 at 100 (*D*) and 1500–100 (*E*) ms. *F–I*, analogous voltage steps over 100 (*F*) or 1800 (*G*) ms and statistics on average currents ± S.E. at 100 (*H*) or 1800 (*I*) ms are presented for coexpression of STIM1 with O1, O3, as well as O1-[Ct-O3] and O3-[Ct-O1].

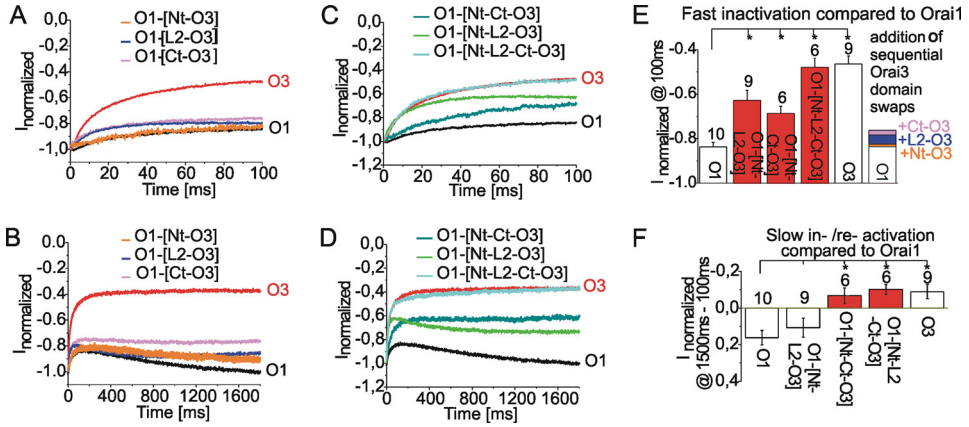

FIGURE 4. **Orai1 chimera with two Orai3 domains swaps exhibit increased fast inactivation.** *A* and *B*, normalized average currents from a voltage step to −82 mV are shown for a coexpression of STIM1 with O1 (*black*), O3 (*red*), as well as O1-[Nt-O3], O1-[Ct-O3], and O1-[L2-O3] for 100 (*A*) or 1800 (*B*) ms. Analogous voltage steps are presented for either O1-[Nt-Ct-O3], O1-[Nt-L2-O3], and O1-[Nt-L2-Ct-O3] for 100 (*C*) or 1800 (*D*) ms. Statistics on normalized average currents ± S.E. are compared for significant difference for O1 to O1-[Nt-L2-O3], O1-[Nt-Ct-O3], O1-[Nt-L2-Ct-O3], and O3 at 100 (*E*) and 1500–100 (*F*) ms. An addition of normalized average currents of O1-[Nt-O3], O1-[L2-O3], and O1-[Ct-O3] are shown at 100 ms included in *E*.

either suggest a further Orai3-specific site fundamental for fast inactivation or point to a cooperative interplay of several gating domains. The unique current profile of O3-[L2-O1] favors the latter hypothesis (see Fig. 2*C*) consistent with the notion that the impact of a transferred domain has to be seen within the context of the overall channel complex. To gain insight into a possibly concerted action of the various cytosolic regions, we generated Orai1 chimeras with double substitutions of Orai3. Indeed, Orai1 with the N terminus and second loop of Orai3 (Orai1-[Nt-L2-O3]) exhibited significantly increased fast inactivation centered between that of the wild-type channels (Fig. 4, *C* and *E*) together with an Orai1-like reactivation (Fig. 4, *D* and *F*). The unaltered reactivation was surprising as both chimeras with a single substitution tended to show a diminished reactivation. Orai1 with both the N and C terminus of Orai3 (Orai1-[Nt-Ct-O3]) also yielded significantly increased fast inactivation (Fig. 4, *C* and *E*) and lacked reactivation (Fig. 4, *D* and *F*). It seems that either the second loop or C terminus together with the N terminus of Orai3 was capable to markedly increase fast inactivation. Moreover, substitution of all three cytsolic domains in Orai1 (O1-[Nt-L2-Ct-O3]) by those of Orai3 induced almost identical gating characteristic as observed with

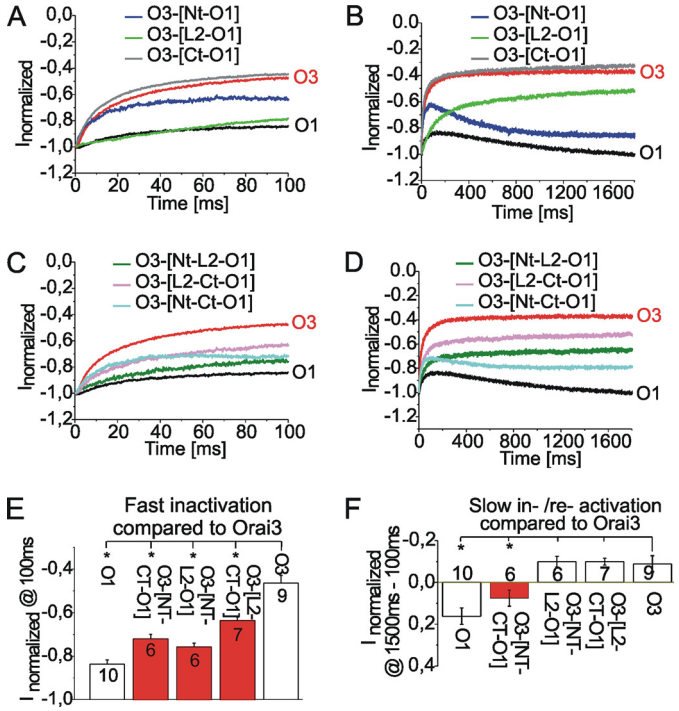

FIGURE 5. **Orai3 chimera with two Orai1 domains swaps show reduced fast inactivation.** *A* and *B*, normalized average currents from a voltage step to −82 mV are shown for a coexpression of STIM1 with O1 (*black*), O3 (*red*), as well as O3-[Nt-O1], O3-[L2-O1], and O3-[Ct-O1] for 100 (*A*) or 1800 (*B*) ms. Analogous voltage steps are presented for either O3-[Nt-L2-O1], O3-[Nt-Ct-O1], and O3-[L2-Ct-O1] for 100 (*C*) or 1800 (*D*) ms. Statistics on normalized average currents ± S.E. of O1, O3-[Nt-Ct-O1], O3-[Nt-L2-O1], and O3-[Ct-L2-O1] are compared for significant difference with O3 at 100 (*E*) and 1500–100 (*F*) ms.

wild-type Orai3 (Fig. 4, *C–F*). In line, similar inactivation profiles of wild-type Orai3 and O1-[Nt-L2-Ct-O3] were also observed in a Ba^{2+}-containing bath solution (supplemental Fig S4, *A* and *B*).

Remarkably, when we calculated the overall increase in fast inactivation obtained in each of the single substituted N or C terminus or second loop Orai1 chimera, altogether it would account for just ~23% of that of wild-type Orai3 (Fig. 4*E*). Hence, our results suggest that a positive cooperative interplay of the N- and C termini together with the second loop of Orai3 can induce drastically stronger fast inactivation of Orai1 than expected from the single domain swaps.

To exclude that these results are blurred by variations of the STIM1 to Orai chimera expression levels (24), we re-examined two Orai1 key constructs with a DNA amount decreased by a factor of two and doubled that of STIM1. We observed a similar inactivation profile for Orai1-[Nt-L2-O3] (supplemental Fig. S4, *C, D, G,* and *H*) as well as Orai1-[Nt-L2-Ct-O3] (supplemental Fig S4, *E–H*) in comparison with a corresponding 1:1 DNA amount of these constructs. Although we do not exclude a general effect of larger variations of STIM1 to Orai expression as reported previously (24), a significant effect in the present study is highly unlikely, in line with our previous results (17).

Next, we examined Orai3 chimeras with double swaps of intracellular Orai1 strands. Substitutions of single Orai1 domains as already shown in the previous figures were depicted for a better comparison in Fig. 5, *A* and *B*. A decrease in fast inactivation was observed for O3-[Nt-O1] and O3-[L2-O1] with a conferred reactivation and increased slow inactivation phase, respectively, whereas only O3-[Ct-O1] retained the typical Orai3 gating characteristics. Both Orai3 double-exchange chimeras containing the second loop with either N or C terminus of Orai1 (O3-[Nt-L2-O1]; O3-[L2-Ct-O1]) showed a decrease of fast inactivation (Fig. 5, *C* and *E*), while retaining a slow inactivation phase similar to that of wild-type Orai3 (Fig. 5, *D* and *F*). An Orai3 chimera with N- and C-terminal domains of Orai1 (Orai3-[Nt-Ct-O1]) also exhibited attenuated fast inactivation but obtained a reactivation phase reminiscent of Orai1 (Fig. 5, *C–F*). Unfortunately, an exchange of all three cytosolic Orai1 domains in Orai3 yielded a construct that exhibited intracellular localization and thus prevented analysis of its gating properties. It is interesting to note that in the case of Orai3 chimeras, single domain swaps with Orai1 N terminus or its second loop appeared more effective when compared with effects observed with the reciprocal Orai1 chimeras. Nevertheless, any combination of two, cytosolic Orai1 domains transferred into Orai3 decreased fast inactivation in comparison to wild-type Orai3. Strikingly, although an exchange of the C terminus alone failed to affect inactivation profiles, a combination with Orai1 N terminus conferred a cooperative effect onto Orai3 chimera by strongly decreasing its fast inactivation.

Identical Cytosolic Domains on Distinct Orai1 or Orai3 Backbone—We compared gating characteristics of Orai1 and Orai3 chimeras that comprise identical N/C termini and second loops, in an attempt to estimate the contribution of the Orai backbone for gating. Without an impact of the respective Orai1/Orai3 backbone (Fig. 6), one would expect that identical cytosolic domains might yield similar gating characteristics that are typically found between those of the wild-type channels. This was only true for two of the examined domain combinations (Fig. 6, *C* and *D*). Fast inactivation of Orai1/3 chimeras with three identical, cytosolic domains was in most cases stronger when the backbone of the protein originates from Orai3 (Fig. 6) with O3-[L2-O1] as the only exception. An additional nonconserved site within Orai3 backbone that might contribute to the observed faster inactivation comprises the unique extension in the third extracellular loop (see Fig. 3, *A*, *B*, and *D*). Additionally, an involvement of the first extracellular loop in fast inactivation has been ascribed to three aspartates in Orai1 (13). Two of these aspartates are glutamates in wild-type Orai3 (supplemental Fig. S5*A*). However, neither an Orai3-E85D-E89D nor Orai1-D110E-A111S-D114E mutant showed a significant change in their gating characteristics (supplemental Fig. S5, *B–E*), rendering the first loop unlikely for mediating faster inactivation of the Orai3 backbone.

Regarding the reactivation phase, Orai1/Orai3 chimeras containing the same combination of cytosolic (Nt, L2, and Ct) domains typically reactivated more robustly when the Orai backbone descended from Orai1 (Fig. 6). It is therefore likely that the reactivation phase involves additional Orai1 backbone structures. Remarkably, the Orai1-[L2-Ct-O3] yielded unique gating characteristics when compared with the analogous Orai3 chimera and exhibited a profound activation phase with the initial fast inactivation completely lacking (Fig. 6*B*). Further Orai subtype specific inactivation/reactivation domains might

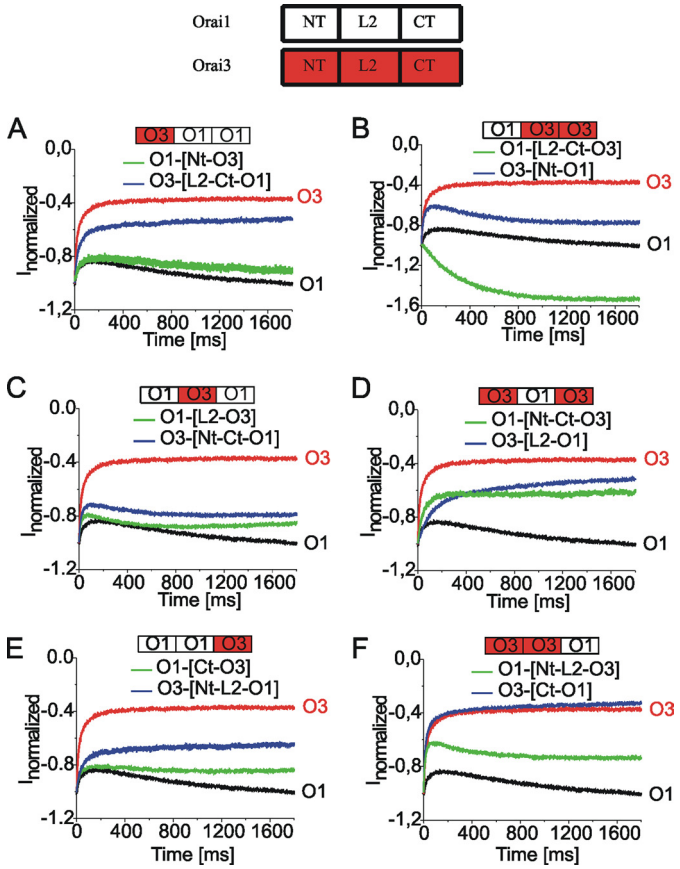

FIGURE 6. **Gating of Orai1 and Orai3 chimera with identical combinations of cytosolic strands.** *A*, normalized average currents from a voltage step to −82 mV are shown for a coexpression of STIM1 with O1 (*black*), O3 (*red*), as well as O1-[Nt-O1] and O3-[L2-Ct-O1] for 1800 ms. Analogous voltage steps compare O1-[L2-Ct-O3] and O3-[Nt-O1] (*B*), O1-[L2-O3] and O3-[Nt-Ct-O1] (*C*), O1-[Nt-Ct-O3] and O3-[L2-O1] (*D*), O1-[Ct-O3] and O3-[Nt-L2-O1] (*E*) as well as O1-[Nt-L2-O3] and O3-[Ct-O1] (*F*).

be discovered within the transmembrane domains that were not analyzed in this study.

DISCUSSION

Domain swapping between Orai1 and Orai3 revealed novel subtype-specific sites determining inactivation/reactivation phases of the Orai gating. Moreover, extending single to multi-domain swaps uncovered a strong cooperative interplay of the cytosolic regions for the fast inactivation process.

Among the single domain exchanges, the N terminus of Orai1 conferred a slow reactivation in an Orai3 chimera. The reciprocal construct (O1-[Nt-O3]), or deletions of proline/arginine-rich regions within the Orai1 N terminus yielded blunted reactivation compared with wild-type Orai1 consistent with a role of the Orai1 N-terminal domain in the reactivation phase. Yuan *et al.* (7) has observed decreased, currents of Orai1 mutants with alanine substitutions within the first (Orai1-P3A-P5A) or second (Orai1-P39A-P40A) proline-rich region that might be compatible with an altered gating process. The proline/arginine-rich regions of the Orai1 N terminus were also identified here as key sites for mediating reactivation gating.

The second loop represents a central gating domain that has been reported to function as an inactivation particle (15). An Orai3 chimera with the second loop of Orai1 depicted a drastically slowed fast inactivation, similar to that of wild-type Orai1, followed by a unique slow inactivation. In contrast, the second loop of Orai3 failed to increase fast inactivation in an Orai1 chimera, which was taken as a first hint that a cytosolic gating domain might not work independently within the overall channel complex. Among the extracellular loops, the region we discovered here within the third loop of Orai3 might play a role for subtype-specific fast inactivation beyond a more general function of the first extracellular loop for Orai gating (13).

Orai3 with the C terminus of Orai1 or its reciprocal chimera did not exhibit a significantly altered gating characteristic. Robust fast inactivation of Orai3 currents has been attributed to three glutamates in the C terminus of the protein (7). As our C-terminal O1-[Ct-O3] chimera lacked an impact on the inactivation profile, this might be taken as a further indication for an interplay of domains required for subtype-specific gating.

In summary, all three Orai1 chimeras each with a single cytosolic strand of Orai3 lacked a significant increase in fast inactivation. On the contrary, double-swap Orai1 chimeras with the N terminus together with the second loop or the C terminus of Orai3 showed substantially increased fast inactivation centered between those of wild-type channels. Moreover, an Orai1 chimera with both the N and C termini as well as the second loop of Orai3 exhibited an Orai3-like inactivation profile, demonstrating the requirement for a cooperative interplay of these three cytosolic domains to fully confer Orai3-gating characteristics.

Two of the Orai3 chimeras with single Orai1 domain swaps (N terminus or second loop) displayed already part of Orai1-like gating characteristics. Exchange of the C-terminal domain of Orai3 alone failed to affect gating characteristics, whereas its combination with the N terminus of Orai1 robustly decreased fast inactivation consistent with a cooperative interplay as observed above with Orai1 chimeras.

In conclusion, we propose a model for Orai gating that is based on a cooperative interplay among the cytosolic N and C termini as well as the second loop. A functional linkage between the N and C terminus is consistent with the reported interaction of STIM1 with both strands (6), but the second loop has so far been considered as a more independent inactivation domain (15). The results obtained here indicate that in particular the second loop of Orai3 requires possible allosteric coupling with N/C-terminal Orai3 domains to accomplish Orai3-specific fast inactivation. Accordingly, the presence of the second loop of Orai1 in an Orai3 chimera efficiently disturbed cooperative interplay with the cytosolic N and C termini, thereby reducing the extent of fast inactivation. STIM1 expression levels have been reported (24) to affect inactivation characteristics, yet might not have significantly contributed to the various gating characteristics observed in this study. Although the role of STIM1 in regulating inactivation/reactivation processes is only partially understood (14, 16, 17), STIM1 might have an impact on gating properties in a more dynamic way by altering the extent of its coupling with Orai via concurrent Orai N-terminal interactions with the Ca^{2+}-binding proteins calmodulin (14). However, our results suggest that Stim1 and CaM play a general role in fast inactivation and less likely account for Orai subtype-specific gating. In this scenario of a dynamic protein assembly

within the whole Orai channel complex, our results demonstrate cooperativeness of cytosolic domains for determining Orai subtype-specific gating and await structural resolution for further promoting our understanding of the intricate Orai/STIM1 gating machinery.

Acknowledgment—We thank S. Buchegger for excellent technical assistance.

REFERENCES

1. Parekh, A. B., and Putney, J. W., Jr. (2005) *Physiol. Rev.* **85,** 757–810
2. Roos, J., DiGregorio, P. J., Yeromin, A. V., Ohlsen, K., Lioudyno, M., Zhang, S., Safrina, O., Kozak, J. A., Wagner, S. L., Cahalan, M. D., Veliçelebi, G., and Stauderman, K. A. (2005) *J. Cell Biol.* **169,** 435–445
3. Liou, J., Kim, M. L., Heo, W. D., Jones, J. T., Myers, J. W., Ferrell, J. E., Jr., and Meyer, T. (2005) *Curr. Biol.* **15,** 1235–1241
4. Luik, R. M., Wang, B., Prakriya, M., Wu, M. M., and Lewis, R. S. (2008) *Nature* **454,** 538–542
5. Muik, M., Frischauf, I., Derler, I., Fahrner, M., Bergsmann, J., Eder, P., Schindl, R., Hesch, C., Polzinger, B., Fritsch, R., Kahr, H., Madl, J., Gruber, H., Groschner, K., and Romanin, C. (2008) *J. Biol. Chem.* **283,** 8014–8022
6. Park, C. Y., Hoover, P. J., Mullins, F. M., Bachhawat, P., Covington, E. D., Raunser, S., Walz, T., Garcia, K. C., Dolmetsch, R. E., and Lewis, R. S. (2009) *Cell* **136,** 876–890
7. Yuan, J. P., Zeng, W., Dorwart, M. R., Choi, Y. J., Worley, P. F., and Muallem, S. (2009) *Nat. Cell Biol.* **11,** 337–343
8. Muik, M., Fahrner, M., Derler, I., Schindl, R., Bergsmann, J., Frischauf, I., Groschner, K., and Romanin, C. (2009) *J. Biol. Chem.* **284,** 8421–8426
9. Hoth, M., and Penner, R. (1993) *J. Physiol.* **465,** 359–386
10. Zweifach, A., and Lewis, R. S. (1995) *J. Gen. Physiol.* **105,** 209–226
11. Lis, A., Peinelt, C., Beck, A., Parvez, S., Monteilh-Zoller, M., Fleig, A., and Penner, R. (2007) *Curr. Biol.* **17,** 794–800
12. Schindl, R., Frischauf, I., Bergsmann, J., Muik, M., Derler, I., Lackner, B., Groschner, K., and Romanin, C. (2009) *Proc. Natl. Acad. Sci. U.S.A.* **106,** 19623–19628
13. Yamashita, M., Navarro-Borelly, L., McNally, B. A., and Prakriya, M. (2007) *J. Gen. Physiol.* **130,** 525–540
14. Mullins, F. M., Park, C. Y., Dolmetsch, R. E., and Lewis, R. S. (2009) *Proc. Natl. Acad. Sci. U.S.A.* **106,** 15495–15500
15. Srikanth, S., Jung, H. J., Ribalet, B., and Gwack, Y. (2010) *J. Biol. Chem.* **285,** 5066–5075
16. Lee, K. P., Yuan, J. P., Zeng, W., So, I., Worley, P. F., and Muallem, S. (2009) *Proc. Natl. Acad. Sci. U.S.A.* **106,** 14687–14692
17. Derler, I., Fahrner, M., Muik, M., Lackner, B., Schindl, R., Groschner, K., and Romanin, C. (2009) *J. Biol. Chem.* **284,** 24933–24938
18. Schindl, R., Bergsmann, J., Frischauf, I., Derler, I., Fahrner, M., Muik, M., Fritsch, R., Groschner, K., and Romanin, C. (2008) *J. Biol. Chem.* **283,** 20261–20267
19. Singh, A., Hamedinger, D., Hoda, J. C., Gebhart, M., Koschak, A., Romanin, C., and Striessnig, J. (2006) *Nat. Neurosci.* **9,** 1108–1116
20. Derler, I., Hofbauer, M., Kahr, H., Fritsch, R., Muik, M., Kepplinger, K., Hack, M. E., Moritz, S., Schindl, R., Groschner, K., and Romanin, C. (2006) *J. Physiol.* **577,** 31–44
21. Xia, Z., and Liu, Y. (2001) *Biophys. J.* **81,** 2395–2402
22. Berney, C., and Danuser, G. (2003) *Biophys. J.* **84,** 3992–4010
23. Frischauf, I., Muik, M., Derler, I., Bergsmann, J., Fahrner, M., Schindl, R., Groschner, K., and Romanin, C. (2009) *J. Biol. Chem.* **284,** 21696–21706
24. Scrimgeour, N., Litjens, T., Ma, L., Barritt, G. J., and Rychkov, G. Y. (2009) *J. Physiol.* **587,** 2903–2918